

Modern Physics Letters A
 © World Scientific Publishing Company

B PHYSICS ON THE LATTICE: PRESENT AND FUTURE

MATTHEW WINGATE

*Institute for Nuclear Theory, University of Washington, Box 351550
 Seattle, Washington, United States
 wingate@phys.washington.edu*

Recent experimental measurements and lattice QCD calculations are now reaching the precision (and accuracy) needed to over-constrain the CKM parameters $\bar{\rho}$ and $\bar{\eta}$. In this brief review, I discuss the current status of lattice QCD calculations needed to connect the experimental measurements of B meson properties to quark flavor-changing parameters. Special attention is given to $B \rightarrow \pi \ell \nu$, which is becoming a competitive way to determine $|V_{ub}|$, and to $B^0 - \bar{B}^0$ mixings, which now include reliable extrapolation to the physical light quark mass. The combination of the recent measurement of the B_s mass difference and current lattice calculations dramatically reduces the uncertainty in $|V_{td}|$. I present an outlook for reducing dominant lattice QCD uncertainties entering CKM fits, and I remark on lattice calculations for other decay channels.

Keywords: CKM matrix; quark flavor; lattice QCD; B mesons.

PACS Nos.: 12.38.Gc, 13.20.He, 14.40.Nd

1. Introduction

The main motivation for studying the properties of B mesons is to understand how quarks change their flavor. Is the Cabibbo-Kobayashi-Maskawa (CKM) mechanism enough to describe flavor-changing processes, or can we see the effects of new physics?

Even with the extraordinary effort made by the B factories, we presently see no cracks in the CKM model. This allows us to eliminate or tightly constrain many new physics models, afflicting them with a so-called flavor problem. Continued agreement of experiment with the CKM model will force us to explain the minimal flavor violation. Better yet, fissures will appear and possibly favor one new model over another. As usual in particle physics, this type of indirect search complements and guides direct searches.

Since quarks are confined inside hadrons, precise and accurate theoretical calculations are necessary to connect the experimental measurements of meson decay and mixing to the fundamental quark couplings. Many quantities important for studying quark flavor are calculated using lattice QCD (LQCD). This brief review focuses on calculations of B decays and mixings. Sec. 2 is an overview of the methodology.

Semileptonic decays like $B \rightarrow \pi \ell \nu$ and $B \rightarrow D \ell \nu$ provide information about how the b quark decays to a u and c quark by W emission. Since these decays

2 *Matthew Wingate*

proceed dominantly through tree diagrams, they allow one to determine the CKM matrix elements $|V_{ub}|$ and $|V_{cb}|$, given clean experimental measurement of decay rates and reliable theoretical calculation of hadronic matrix elements. $B \rightarrow \pi \ell \nu$ decays were hard to use to determine $|V_{ub}|$ because of small branching fractions and large theoretical uncertainties. In the past year both experiment and theory have improved greatly, the latter through unquenched LQCD calculations. Section 3 reviews this important development, gives an update on $B \rightarrow D \ell \nu$, and discusses the difficulties and possibilities for lattice calculations relevant to other semileptonic decays which might also determine $|V_{ub}|$.

Mixing between neutral mesons proceeds through loop diagrams to which new physics particles can contribute. It is possible that new physics could be discovered by assuming that only Standard Model particles contribute and showing that the resulting CKM parameters do not agree with the CKM parameters obtained from tree-level decays. Both $K^0 - \bar{K}^0$ and $B^0 - \bar{B}^0$ oscillations provide important ways to search for deviations from the CKM mechanism. As in the case of semileptonic decays, calculations of hadronic matrix elements are necessary in order to learn about quark level processes from experimental measurements of mass and lifetime differences. Section 4 describes recent progress made using LQCD in concert with new experimental results.

Rare decays, like $B \rightarrow K^* \gamma$, occur through loop diagrams called penguins. In principle lattice QCD can also provide reliable calculations of the relevant hadronic matrix elements for these processes. Some technical difficulties facing LQCD contributions to rare decays are explained in Section 5.

This review closes with the lattice prediction and subsequent experimental measurement of the B_c mass (Sec. 6) and a few concluding remarks (Sec. 7).

2. Overview of Methodology

To many people lattice QCD is a black box into which one puts the strong coupling constant and quark masses and out of which one obtains the properties of hadrons. If only that were so. Those people who live inside the box see LQCD is a method for numerically integrating Euclidean spacetime path integrals, valid even when there are no small parameters about which to form a perturbation theory. Communication between those living inside and outside the box is imperative if progress is to be made. Here I discuss some details of LQCD that will facilitate later discussions about recent progress and future improvements and obstacles. Interested readers can find more detailed treatments elsewhere.¹

Expectation values of observables are given by integrals over all possible field configurations. For example the expectation value of operator O is given by

$$\langle O \rangle = \frac{1}{Z} \int \mathcal{D}\psi \mathcal{D}\bar{\psi} \mathcal{D}U O[\psi, \bar{\psi}, U] e^{-S[\psi, \bar{\psi}, U]} \quad (1)$$

where the $\psi, \bar{\psi}$ represent the quark, antiquark fields and U represents the glue field. The action S is the integral over space and imaginary time of the QCD Lagrangian.

Lattice QCD provides a method for numerically evaluating path integrals from first principles. The integral is made finite by discretizing spacetime. The presence of the damped exponential in (1) means that only a small set of field configurations will contribute to the path integral. This is analogous to studying a classical gas: the important configurations of particle positions and velocities are a small fraction of the multitude of possible configurations, most of which give exponentially small contributions to statistical traces over microstates.

The way that fermion antisymmetry is represented in path integrals causes great difficulty for numerical methods. The quark and antiquark fields are valued over the field of anticommuting complex numbers (Grassmann numbers) instead of the usual complex numbers. This is a formal construction which generally does not permit numerical evaluation. Luckily, if the action is quadratic in the fermion fields, $S_f = \bar{\psi} Q \psi$, the integral over fermion fields can be done exactly, yielding a determinant, $\det Q$. For example, the vacuum expectation value of a quark bilinear is given by

$$\langle \bar{\psi} \Gamma \psi \rangle = \int \mathcal{D}U \frac{\delta}{\delta \bar{\zeta}} \Gamma \frac{\delta}{\delta \zeta} e^{-\bar{\zeta} Q^{-1}[U] \zeta} \det Q[U] e^{-S_g[U]} \Big|_{\zeta, \bar{\zeta} \rightarrow 0} \quad (2)$$

where Γ is a product of Dirac γ matrices and the $\zeta, \bar{\zeta}$ act as fermion sources. The quantities calculated for B physics results, 2- and 3-point correlation functions, are straightforward generalizations of (2). The penalty we pay for this formal integration is that a nonlocal updating algorithm must be used to do importance sampling. A necessary step involves inverting a matrix which becomes singular as up/down quark masses are decreased from artificially heavy to their physical values.

Writing (2) in detail allows us to define some terminology. Note the 2 places the quark matrix Q appears in (2). These correspond to 2 distinct steps in a lattice QCD calculation. The determinant of Q is included in the probability weight during the generation of typical, important glue field configurations. The resulting collection of configurations is then stored and later used to calculate ensemble averages of operators. In the case of fermionic operators, the inverse of Q is computed during this ensemble averaging. The term “sea quarks” refers to contributions of $\det Q$ to the importance sampling and “valence quarks” refers to the fully dressed propagators Q^{-1} . Logistically nothing prevents one from using different quark mass values for the sea and valence quark steps. This procedure is called “partial quenching” and is useful since the generation of configurations is much more costly than the calculation of quark propagators.^{2,3} Full QCD is in some sense a special case of partially quenched QCD where $m_{\text{sea}} = m_{\text{valence}}$.

The last important point is that the discretization Q of the Dirac operator, $\mathcal{D} + m$, is not unique. The choice of discretization has consequences for the systematic uncertainties in numerical results and for the computational expense. One discretization, the improved staggered quark action, permits numerical calculation with sea (and valence) quark masses down to 1/10 the strange quark mass. (The cost of the calculations increases rapidly as m decreases.) Ensembles of configurations which include effects of 2+1 flavors of sea quarks using an improved staggered

4 *Matthew Wingate*

action, have been generated and made public by the MILC collaboration.⁴ The effects of using light sea quarks are dramatic: cleanly computable quantities, many of which the quenched approximation got wrong by over 10%, agree nicely with experiment.⁵ Calculations with other quark discretizations are desirable (1) to further check the “fourth-root” algorithmic trick one needs with staggered quarks to obtain 2 + 1 sea quark flavors;⁶ (2) to avoid the complications staggering creates in calculations of light baryon properties.^{7,8,9} Unquenched calculations with improved Wilson quarks and domain wall quarks are making steady progress. However, their advantages are tempered by having to extrapolate using data with heavier quark masses, perhaps without sufficient theoretical control. Checks similar to those done for staggered fermions are needed for non-staggered actions to demonstrate that the extrapolations to physical sea quark masses are under control.

3. Semileptonic Decays and CKM Matrix Elements

Semileptonic decays, where quark flavor is changed by emission of a single W boson, provide direct access to the first 2 rows of the CKM matrix. It is useful to focus on these tree-level decays separately from processes which begin at 1-loop level because new physics particles generally should affect the latter more than the former.

In order to use experimental measurements of semileptonic decays to determine the CKM matrix elements, one needs accurate calculations of the weak current between hadronic initial and final states. In the next section the lattice calculations needed for $|V_{cb}|$ and $|V_{ub}|$ are discussed (as are $|V_{cs}|$ and $|V_{cd}|$, briefly). The mixing calculations relevant for $|V_{td}|$ and $|V_{ts}|$ are discussed in Sec. 4. This brief review will not cover calculations for $|V_{us}|$ using lattice QCD, although there has been significant recent progress, using the leptonic decay constants^{10,11} or the semileptonic form factor.^{12,13,14,15} Finally, $|V_{ud}|$ is most precisely determined from nuclear and neutron beta decays without needing lattice QCD.¹⁶

3.1. $B \rightarrow D^{(*)}\ell\nu$

Presently, the most precise determination of $|V_{cb}|$ comes from inclusive measurements.¹⁷ Improvements in lattice QCD calculations will help to reduce the uncertainties in determinations from exclusive decays, especially $B \rightarrow D^{*}\ell\nu$. Regardless of which method is most precise, cross-checks are important to truly over-constrain the CKM model.

The matrix element $|V_{cb}|$ may be determined from exclusive semileptonic B decays to the D or D^{*} by fitting the experimental measurements of the differential partial decay width to

$$\frac{d\Gamma}{dw}(B \rightarrow D^{(*)}\ell\nu) = \frac{G_F^2 |V_{cb}|^2}{48\pi^3} \mathcal{K}_{B \rightarrow D^{(*)}}(w) \mathcal{F}_{B \rightarrow D^{(*)}}^2(w) \quad (3)$$

where $w = v_B \cdot v_{D^{(*)}}$ is the velocity transfer and $\mathcal{K}_{B \rightarrow D^{(*)}}(w)$ is a known kinematic function of w . The shape of $\mathcal{F}_{B \rightarrow D^{(*)}}(w)$ near $w = 1$ is given by dispersive bounds

and HQET,¹⁸ and experimenters quote measured values for $\mathcal{F}_{B \rightarrow D^{(*)}}(1)|V_{cb}|$. The overall normalization can then be computed using lattice QCD.

The LQCD calculation can be made very precise by constructing a double ratio of matrix elements, wherein many uncertainties cancel.¹⁹ Preliminary unquenched results give $\mathcal{F}_{B \rightarrow D}(1) = 1.074(18)(16)$, where the first error are statistical and the second is a combination of 1% systematic errors.²⁰ Combining this with the Winter 2006 experimental average²¹ gives $|V_{cb}| = (39.7 \pm 4.2)_{\text{exp}} \pm 0.9_{\text{latt}} \times 10^{-3}$.

While for $B \rightarrow D\ell\nu$ the dominant uncertainty lies on the experimental side, the experimental error is 2% for $B \rightarrow D^*\ell\nu$. Furthermore, Luke's theorem says the heavy quark effective theory errors should also be smaller for the latter decay. One hiccup is that the LQCD extrapolation of $\mathcal{F}_{B \rightarrow D^*}(1)$ from the input light quark mass to the physical light quark mass passes through the $D^* \rightarrow D\pi$ threshold. Improved staggered fermion calculations are poised to solve this problem for 2 reasons. First, the calculations are able to be performed within the chiral regime, so that heavy meson chiral perturbation theory can provide a reliable formula for extrapolation. Second, the presence of artificially heavy staggered pions actually smoothes out the cusp in $\mathcal{F}_{B \rightarrow D^*}(1)$ at threshold as seen in staggered chiral perturbation theory.²²

3.2. $B \rightarrow \pi\ell\nu$

Because π and B have the same parity, only the vector part of the weak current mediates $B \rightarrow \pi\ell\nu$. The matrix element can be parameterized by 2 form factors:

$$\langle \pi(p_\pi) | V^\mu | B(p_B) \rangle = f_+(q^2) \left(p_B^\mu + p_\pi^\mu - \frac{m_B^2 - m_\pi^2}{q^2} q^\mu \right) + f_0(q^2) \frac{m_B^2 - m_\pi^2}{q^2} q^\mu. \quad (4)$$

The form factor $f_+(q^2)$ describes the momentum dependence of the differential partial decay rate in the B rest frame by

$$\frac{d\Gamma}{dq^2} = \frac{G_F^2}{24\pi^3} |\vec{p}_\pi|^3 |V_{ub}|^2 |f_+(q^2)|^2. \quad (5)$$

Experiments have measured the $B^0 \rightarrow \pi^- \ell^+ \nu$ branching fraction with impressive precision. $|V_{ub}|$ is determined by integrating f_+ over q^2 . There is presently a lower limit on q^2 below which the lattice calculations incur large discretization errors: the π should not have momentum larger than the inverse lattice spacing. Therefore, theoretical errors are minimized by integrating over $16 \text{ GeV}^2 \leq q^2 \leq q_{\text{max}}^2$ and using the branching fraction with the same momentum cut.²³

Two groups are completing calculations of the $B \rightarrow \pi\ell\nu$ form factors. They both use the MILC configurations, which include effects of 2+1 quark flavors using the improved staggered action. The main difference is the heavy quark formulation: either lattice NRQCD²⁴ or the Fermilab method.¹³ NRQCD is computationally inexpensive but requires the heavy quark mass to be greater than the inverse lattice spacing, precluding charm studies with NRQCD on the MILC lattices. The Fermilab method is valid for all quark masses.

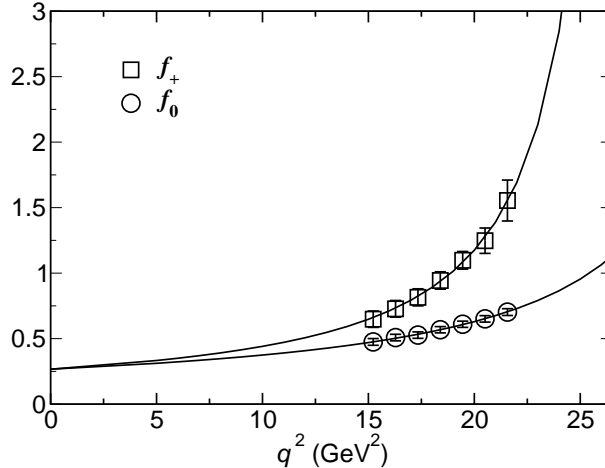


Fig. 1. HPQCD results for the $B \rightarrow \pi$ form factors. The symbols are lattice data after extrapolating the light quark mass to zero, and the curves are fits to the Ball-Zwicky parameterization.

One needs to fit the q^2 dependence of the form factors to a functional form for two reasons. First, to interpolate the finite quark mass lattice data to fixed values of E_π , so that the chiral extrapolation may be performed.²⁵ Second, to facilitate integration of f_+ over a range of q^2 corresponding to the same range for a measured branching ratio, yielding a determination of $|V_{ub}|$. The commonly-used 3-parameter Bećirević-Kaidalov ansatz²⁶ fits the HPQCD lattice data well only after extrapolation to the chiral limit. Instead we use the 4-parameter Bećirević-Kaidalov ansatz advocated by Ball and Zwicky.²⁷

The final HPQCD result is²⁴

$$\frac{1}{|V_{ub}|^2} \int_{16 \text{ GeV}^2}^{q_{\text{max}}^2} dq^2 \frac{d\Gamma}{dq^2} = 1.46 \pm 0.23 \pm 0.27 \text{ ps}^{-1} \quad (6)$$

where the first error is statistical plus chiral extrapolation and the second is other systematics added in quadrature. The dominant source of systematic uncertainty is due to truncating at 1-loop order the perturbative matching between the lattice NRQCD current and the continuum weak vector current. This agrees within errors with the preliminary result using the Fermilab heavy quark action: $|V_{ub}|^{-2} \int_{16 \text{ GeV}^2}^{q_{\text{max}}^2} dq^2 (d\Gamma/dq^2) = 1.83 \pm 0.50 \text{ ps}^{-1}$.²⁰ The dominant error in the latter calculation is due to discretization errors in their heavy quark action. Taking current experimental results for the $B^0 \rightarrow \pi^- \ell^+ \nu$ branching ratio^{28,29,21} and B^0 lifetime¹⁷ along with the HPQCD result (6) yields²⁴

$$|V_{ub}| = (4.22 \pm 0.30_{\text{exp}} \pm 0.34_{\text{stat}} \pm 0.38_{\text{sys}}) \times 10^{-3}. \quad (7)$$

With NRQCD for the heavy quarks, the leading uncertainty comes from the perturbative matching of the lattice currents to the continuum weak current.²⁴ The matching is presently done at 1-loop level. The 2-loop calculation is very involved

and will require automated perturbation theory techniques.³⁰ With the Fermilab heavy quark formulation, there is a conserved current which allows most of the matching to be determined nonperturbatively. The remaining perturbative corrections are tiny, so truncating at 1-loop level is sufficient until other errors are decreased. The leading uncertainty in this case is the discretization error in the heavy quark formulation. The improved action has been worked out,³¹ but an efficient implementation is still under development.

There are several efforts to reduce any systematic uncertainties due to modeling the shape of the form factor. The shape is strongly constrained by unitarity, analyticity and heavy quark effective theory.^{32,33} Plotted against an appropriate variable, the shape of f_+ is consistent with a linear fit.³⁴ Recent analyses^{35,36} make it apparent that LQCD calculations can reduce the uncertainty in $|V_{ub}|$ by more precisely determining the form factor normalization.

We see that determinations of $|V_{ub}|$ from $B \rightarrow \pi\ell\nu$ decays are becoming competitive with the precision from inclusive determinations.³⁷ Using exclusive decays also has the advantage of avoiding the hypothesis of quark-hadron duality which is necessary for inclusive determinations and blunts tests of the CKM model.

3.3. $D \rightarrow \pi\ell\nu$ and $D \rightarrow K\ell\nu$

Even though D decays are outside the scope of this brief review, the recent calculations of semileptonic D form factors have implications for the $B \rightarrow \pi$ form factors, on top of providing determinations of $|V_{cd}|$ and $|V_{cs}|$.³⁸ The lattice calculations are done with a subset of the same MILC configurations discussed above⁴ and use the improved staggered quark action in both the B and D correlation functions.³⁹ The charm quark is treated using the Fermilab formulation, as in the Fermilab/MILC B meson calculations. Given these similarities, the agreement between the lattice calculation of $f_+(q^2)$ for $D \rightarrow K$ and the recent experimental measurement^{40,41} testifies to the validity of the $B \rightarrow \pi$ form factor calculations.

3.4. Other $b \rightarrow u\ell\nu$ Decays and Associated Challenges

Exclusive determinations of $|V_{ub}|$ from other exclusive B decays $B \rightarrow \pi\ell\nu$ are also valuable. Every independent measurement has the potential to play a role in the quest to see new physics through over-constraining the CKM parameters. Even within the Standard Model, it is conceivable that another decay channel will lead to a more precise determination than $B \rightarrow \pi\ell\nu$, provided that lattice QCD can meet some challenges.

Experiments show the $B \rightarrow \rho\ell\nu$ branching fraction to be twice as big as to $\pi\ell\nu$, so its precision is easier to reduce. However, to get an accurate $|V_{ub}|$ the theoretical uncertainties in the form factors must be under control; presently they are not.⁴² The main open problem is the extrapolation of lattice data obtained with quark masses where the ρ is stable through $\rho \rightarrow \pi\pi$ threshold. The firm theoretical ground

provided by chiral perturbation theory for B and π properties becomes quite muddy underneath the ρ .

Experiments have measured $B \rightarrow \eta \ell \nu$.⁴³ The lattice calculation with the η suffers because it is partially a flavor singlet. There are disconnected contributions to the correlation functions where the valence $\bar{q}q$ pair are annihilated then recreated. These are notoriously hard to calculate due to poor signal-to-noise. Nevertheless, these contributions are important to the η propagator due to the anomaly.

The situation may not be as glum for $B \rightarrow \omega \ell \nu$,⁴⁴ which has recently been observed.⁴⁵ The ω is a narrow resonance in contrast to the ρ . Despite being a flavor singlet, violations of the OZI rule are expected to be smaller for the vector ω than for the pseudoscalar η , since the anomaly affects only the latter. LQCD calculations of flavor singlet meson masses support this expectation so far.^{46,47} We should explore in more depth the reliability of calculating the properties of the ω on the lattice and see how far we can push a calculation of the $B \rightarrow \omega$ form factors. If we can truly neglect disconnected contributions to the ω propagator, then the lattice calculation of $B \rightarrow \omega$ form factors would be identical to $B \rightarrow \rho$, with less headache regarding the meson's width. Disconnected contributions are routinely ignored in LQCD calculations of the ϕ meson mass, for example.

4. Mixing and the Search for New Physics

Studying the oscillations of neutral mesons has the potential to expose physics beyond the Standard Model in a way that the semileptonic decays do not. Any new physics entering the semileptonic decays would be a small contribution to the tree-level standard model decays. In contrast oscillations begin at one-loop level in the standard electroweak theory, and new particles can enter directly in those loops. The leading uncertainties so far are theoretical. Nevertheless, with increased precision in lattice calculations and with the new measurement of $B_s^0 - \bar{B}_s^0$ oscillations, the potential to see a breakdown of the CKM model is realistic, even if unrealized presently. This section summarizes the most recent lattice QCD results and prospects for further improvement.

Before turning to the B^0 mixings, let us consider K^0 and D^0 mixings. Neutral kaon mixing is another important window into flavor physics which relies on lattice QCD. The theoretical error presently dominates that constraint on $(\bar{\rho}, \bar{\eta})$. This situation should improve as we see more unquenched calculations of the hadronic matrix element parametrized by B_K .⁴⁸

$D^0 - \bar{D}^0$ mixing proceeds very slowly compared to mixing the K and B systems. In the Standard Model, this is because the top quark mass, more than 40 times m_b , enhances the $\Delta B = 2$ and $\Delta S = 2$ box diagrams compared to $\Delta C = 2$. Of course, rare processes are just the kind one wants to study to discover new physics. As soon as precise experimental measurements can be made, lattice QCD would be valuable in connecting the meson mass and width differences to models of quark flavor-changing interactions. The relevant matrix elements were calculated some

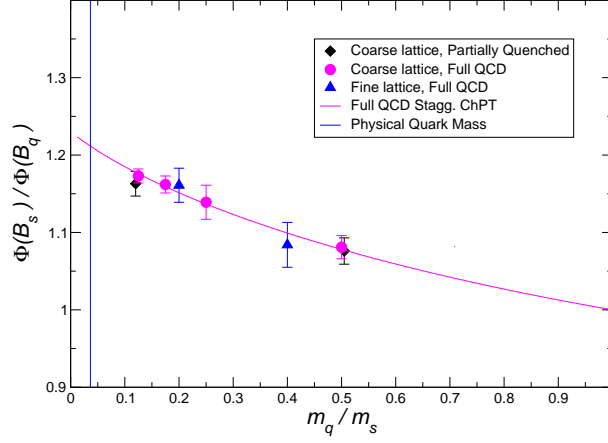


Fig. 2. Ratio of f_{B_s}/f_{B_q} (times $\sqrt{m_{B_s}/m_{B_q}}$) vs. mass of the light quark (in units of the physical strange quark mass).

time ago^{49,50} and should be updated using unquenched configurations and the Fermilab formulation for the charm quark.

4.1. $B^0 - \overline{B^0}$

In the Standard Model $B^0 - \overline{B^0}$ mixing proceeds via 1-loop box diagrams, with the dominant contribution coming from a top quark in the loop. Measurements of the oscillation frequency Δm_d can be used to constrain the CKM matrix element $|V_{td}|$. The relevant hadronic matrix element is conveniently parameterized as

$$\langle \overline{B^0} | (\overline{bd})_{V-A} (\overline{bd})_{V-A} | B^0 \rangle \equiv \frac{8}{3} f_B^2 m_B^2 B_B. \quad (8)$$

This is helpful for two reasons. The leptonic decay constant f_B is simpler to compute in lattice QCD. In addition chiral perturbation theory shows that f_B is more sensitive to the quark mass than B_B , the ratio of the full matrix element to its value in the vacuum saturation approximation.

As discussed above, the LQCD calculations are done with quark masses m_q larger than the physical up/down quark mass. Let's denote the corresponding decay constant by f_{B_q} . In the past, the extrapolation of f_{B_q} to the physical light quark mass was done phenomenologically. Since the lattice data for f_{B_q} are linear in the regime $m_s/2 < m_q < 2m_s$, a linear fit was used for the extrapolation. Chiral perturbation theory gives the m_q dependence of f_{B_q} including logarithmic curvature; however the theory must be used in the small m_q regime, approximately $m_q \leq m_s/2$. The use of improved staggered quarks for the fermion determinant and for the light quark propagator allows LQCD calculations to be performed inside this chiral regime.

The HPQCD collaboration has used the MILC lattices discussed above to calculate f_{B_q} vs. m_q (see Fig. 2). The data are fit using an extension of chiral perturbation theory suitable for staggered fermion calculations.⁵¹ Our result for f_B is $216 \pm 9_{\text{stat}} \pm 20_{\text{sys}}$ MeV.⁵² The leading uncertainty is due to the perturbative matching between the currents in the heavy quark effective theory (lattice NRQCD) and the continuum weak axial vector current, which has been done at 1-loop order.⁵³ As in the case of the $B \rightarrow \pi$ form factors, reducing this uncertainty requires a difficult 2-loop calculation.

Very recently the Belle experiment reported a result $f_B = 176^{(+28)}_{(-23)} \text{stat}^{(+20)}_{(-19)} \text{sys}$ MeV from a first measurement of $B^- \rightarrow \tau^- \bar{\nu}_\tau$ combined with $|V_{ub}|$ from $B \rightarrow X_u \ell \nu$.^{54,21} The confirmation of the LQCD prediction directly speaks to the validity of LQCD calculations for B meson properties, in particular the use of NRQCD heavy quarks, staggered light quarks, and staggered chiral perturbation theory.

In order to further judge the reliability of the lattice QCD calculation of f_B , it is useful to look at the D decay constant. A lattice calculation, which differed from the f_B calculation only in heavy quark action, recently predicted f_D to be $201 \pm 3_{\text{stat}} \pm 17_{\text{sys}}$ MeV,⁵⁵ much more precise than the 20% experimental uncertainty at the time.⁵⁶ Subsequently, CLEO-c found $f_D^{\text{expt}} = 223 \pm 17_{\text{stat}} \pm 3_{\text{sys}}$ MeV from $D^+ \rightarrow \mu^+ \nu$.⁵⁷ This successful prediction by lattice QCD using the same MILC configurations, light quark action, and staggered chiral perturbation theory provides a significant test of the f_B calculation.

The remainder of the hadronic matrix element, B_B , remains to be calculated on the MILC lattices, although preliminary efforts have begun.⁵⁸ The state-of-the-art is still the JLQCD calculation done with improved Wilson fermions.⁵⁹ The same systematic uncertainties affect their result as the HPQCD result for f_B : truncating the perturbative and heavy quark expansions. Since the chiral extrapolation for B_B is milder than for f_B , it is reasonable to expect their result to be close to what will be obtained with lighter quark mass computations. Combining the 2 groups' results one obtains $f_B \sqrt{B_B} = 244 \pm 26$ MeV.⁶⁰ This reduces the uncertainty down to 11% from the previous world average $f_B \sqrt{B_B} = 214 \pm 38$ MeV.⁶¹

Fig. 3a shows the constraint in the $\bar{\rho} - \bar{\eta}$ plane from Δm_d . The improvement indicated by the 2 bands is achieved by reducing the long extrapolation of f_B in light quark mass.

For physics beyond the standard Model, $B^0 - \bar{B}^0$ oscillations may be governed by 4-quark operators with different structure than in (8); this is certainly the case for supersymmetric extensions of the Standard Model.⁶² Therefore, matrix elements of all 5 possible operators should be computed using unquenched lattice QCD, as has been done in the quenched approximation.⁶³

Given the difficulty of 2-loop calculations in lattice perturbation theory, compounded by complexity of heavy quark lattice actions, a fully nonperturbative method would be most welcome. Several such approaches are being investigated.^{64,65,66,67} Only time will tell which of these approaches will first sur-

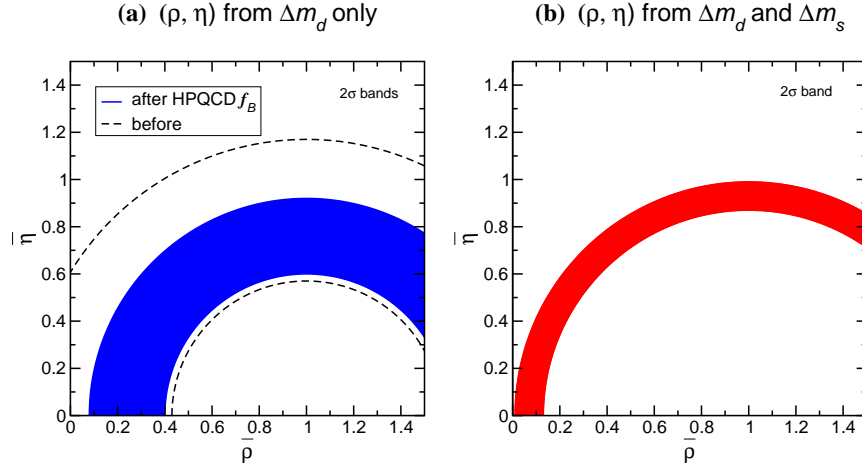


Fig. 3. Constraints (at the 2σ level) on $|V_{td}| = A\lambda^3 \sqrt{(1-\bar{\rho})^2 + \bar{\eta}^2}$. (a) Old and new constraints from Δm_d . (b) Constraint from $\Delta m_d/\Delta m_s$ using the new CDF measurement and recent LQCD improvements.

pass in precision the methods used in present calculations and when that might occur.

4.2. $B_s^0 - \bar{B}_s^0$

Unlike leptonic B , D , and D_s decays, which are merely helicity-suppressed, leptonic B_s decays are forbidden in the Standard Model since they would proceed through a flavor-changing neutral current. Nevertheless, the decay constant $f_{B_s} \equiv \langle 0|A_0|B_s\rangle/m_{B_s}$ is finite and approximately equal to f_B . Again, it provides a useful parameterization of the hadronic matrix element relevant for $B_s^0 - \bar{B}_s^0$ mixing, as in (8).

Very recently, the D0 experiment reported a 2-sided bound on the oscillation frequency $17 \text{ ps}^{-1} < \Delta m_s < 21 \text{ ps}^{-1}$ at the 90% confidence level,⁶⁸ and the CDF collaboration reported a measurement of $\Delta m_s = 17.3^{+0.4}_{-0.2} \text{ ps}^{-1}$.⁶⁹ Some theoretical uncertainties cancel in ratio of the neutral B_s and B oscillation frequencies, so a theoretical calculation of $f_{B_s}^2 B_{B_s}/f_B^2 B_B$ can now provide a much tighter constraint on $|V_{td}|$ than using only nonstrange B oscillations.

The HPQCD result for f_{B_s} is $260 \pm 7_{\text{stat}} \pm 28_{\text{sys}}$ MeV using a nonrelativistic b quark and the MILC lattices described above.⁷⁰ As with f_B , the perturbative matching is the dominant source of systematic uncertainty. This uncertainty largely cancels in the ratio $f_{B_s}/f_B = 1.20 \pm 0.03 \pm 0.01$, where the first uncertainty is statistical error in the correlation functions and in the chiral extrapolation, and the second uncertainty estimates truncated terms in the usual expansions.⁵² Combining

12 *Matthew Wingate*

this ratio with the JLQCD ratio of B factors⁵⁹ yields⁶⁰

$$\frac{f_{B_s}}{f_B} \sqrt{\frac{\hat{B}_{B_s}}{\hat{B}_B}} = 1.210^{+47}_{-35}. \quad (9)$$

Ratios of the B and B_s decay constants and B factors have also been determined in the static limit with 2 flavors of sea quarks using the domain wall fermion action.⁷¹

The constraint obtained by combining the improved LQCD ratio (9) with the new CDF measurement⁶⁹ (and $\lambda = 0.225(1)^{16}$) more than halves the width of the allowed annulus to $\sqrt{(1 - \bar{\rho})^2 + \bar{\eta}^2} = 0.93(3)$, as shown in Fig. 3b.

The $B_s^0 - \bar{B}_s^0$ lifetime difference is also an interesting quantity, but one for which theoretical progress is desirable.⁷² Lattice QCD can contribute by calculating $\langle \bar{B}_s | (\bar{b}s)_{S-P} (\bar{b}s)_{S-P} | B_s \rangle$. A preliminary result from JLQCD was reported some time ago: the ratio of the correct matrix element to the vacuum-saturation approximation was found to be $B_S(m_b) = 0.86(3)(7)$ in the $\overline{\text{MS}}$ scheme.⁷³

5. Penguins and Associated Challenges

5.1. Rare B Decays

Lattice QCD could provide input to tests of the CKM model using radiative decays $B \rightarrow V\gamma$. Belle has measured branching fractions for $B \rightarrow (\rho/\omega)\gamma$.⁷⁴ Many new flavor models predict enhanced $B \rightarrow K^*\gamma$ decays. While LQCD input for the relevant form factor is highly desirable, serious technical problems must first be solved.⁷⁵ At the physical point, $q^2 = 0$, calculations done in the B rest frame have a final state hadron with momentum much greater than the inverse lattice spacing, ensuring lattice artifacts dominate. The challenge in working with small q^2 with present methods, i.e. in the B rest frame, is that lattice artifacts dominate when the light meson's momentum becomes comparable to the inverse lattice spacing. Efforts are underway to formulate and employ lattice NRQCD in a frame where the B is moving, thus keeping the light meson's momentum small compared to the inverse lattice spacing.^{76,77,78,79,80} In addition, one again has to face questions regarding extrapolating lattice data through thresholds.

Lattice QCD can play a more immediate role in rare B decays by calculating the form factors for $B \rightarrow K^{(*)\ell^+\ell^-}$ decays. Branching fractions apparently agree with the Standard Model predictions,^{81,82,83} but these predictions rely on sum rule determinations for the form factors. As the experimental precision increases, the burden will turn to LQCD to reduce theoretical uncertainty. In fact, the LQCD calculation for the most important $B \rightarrow K\ell^+\ell^-$ matrix element (within the Standard Model), $\langle K | \bar{s}\gamma_\mu b | B \rangle$, is very similar to the $B \rightarrow \pi\ell\nu$ form factor calculations discussed above (Sec. 3).⁸⁴ The only difference is that the mass of the strange quark should be held fixed as the mass of the spectator light quark is chirally extrapolated. $B \rightarrow K^*\ell^+\ell^-$ would be worth exploring as well.

5.2. $\Delta B = 0$ Matrix Elements

Lattice QCD can improve theoretical calculations of the B meson lifetimes through calculations of $\langle B | \mathcal{O}_{\Delta B=0} | B \rangle$, where the \mathcal{O} represents four $\Delta B = 0$ 4-quark operators.⁸⁵ Within the context of a certain flavor physics model, e.g. the CKM model, the experimental B meson (and Λ_b) lifetimes can be used to test the validity of the quark-hadron duality required to express the lifetimes in terms of those matrix elements. Two main challenges obstruct this calculation; these are familiar from LQCD calculations of $\langle \pi | \mathcal{O}_{\Delta S=1} | K \rangle$ for $K \rightarrow \pi\pi$. First, these operators mix with lower dimensional ones, and a power-law subtraction must be performed. Second, it is very difficult technically to calculate the contribution to the matrix element when the light quark and antiquark in $\mathcal{O}(x)$ are contracted to form a propagator $G(x, x)$. These challenges are not insurmountable and deserve to be met. An exploratory study was reported some time ago.⁸⁶

These calculations would have impact beyond the B meson lifetimes themselves. Again using quark-hadron duality and the optical theorem, LQCD calculations of the matrix elements of two $\Delta B = 0$ 4-quark operators would be helpful in improving the determination of $|V_{ub}|$ from $\overline{B} \rightarrow X_u \ell^- \bar{\nu}$.⁸⁷

6. Charmed Beauty

Using the MILC configurations discussed above, a very precise prediction for the B_c mass was recently obtained: $m_{B_c}^{\text{latt}} = 6304 \pm 12^{+18}_{-0}$ MeV.⁸⁸ This lattice QCD prediction has since been confirmed by experiment, $m_{B_c}^{\text{expt}} = 6287.0 \pm 4.8 \pm 1.1$ MeV.⁸⁹ The correlation function necessary for the calculation used a nonrelativistic action for the b quark and the Fermilab relativistic action for the c quark. Consequently, the agreement between LQCD and experiment further supports the use of both heavy quark formulations and improved staggered sea quarks.

7. Conclusions

The past 2 years have been especially fruitful for the interplay between lattice QCD and heavy flavor physics, with sharp improvements in LQCD and experimental results. Precise measurements of $B \rightarrow \pi \ell \nu$ decay combined with LQCD calculations of $B \rightarrow \pi$ form factors are making exclusive determinations of $|V_{ub}|$ as precise as inclusive determinations, with prospects for further improvement. Employing an improved staggered quark action, LQCD calculations can be done with light quark masses inside the chiral regime. The resulting prediction of f_B has since been confirmed with the first measurement of $B \rightarrow \tau \nu$ decay. Furthermore, removing chiral extrapolation and quenching errors from the ratio f_{B_s}/f_B combines with the first measurements of Δm_s to drastically improve the precision of $|V_{td}|$. The orthogonality of the $|V_{td}|$ and $\sin 2\beta$ constraints on $(\bar{\rho}, \bar{\eta})$ creates a small target for other CKM constraints to hit. Most of us hope the Cabibbo-Kobayashi-Maskawa trio's aim will eventually fail, cracking the Standard Model. If not, the burden is on

14 *Matthew Wingate*

the model builders to explain the remarkable craftsmanship of the CKM mechanism.

Acknowledgments

The work was supported by DOE grant number DE-FG02-00ER41132. I am grateful to my collaborators C. T. H. Davies, A. Gray, E. Gulez, G. P. Lepage, and J. Shigemitsu. I thank L. Lellouch, C.-J. D. Lin, S. Sharpe and A. Soni for discussions.

References

1. E.g. see M. Wingate, eConf **C0406271**, TUET01 (2004) [arXiv:hep-ph/0409099]; T. DeGrand, Int. J. Mod. Phys. A **19**, 1337 (2004) [arXiv:hep-ph/0312241]; A. S. Kronfeld, arXiv:hep-lat/0205021.
2. S. R. Sharpe and N. Shores, Phys. Rev. D **62**, 094503 (2000).
3. A. G. Cohen, D. B. Kaplan and A. E. Nelson, JHEP **9911**, 027 (1999).
4. C. W. Bernard *et al.*, Phys. Rev. D **64**, 054506 (2001) [arXiv:hep-lat/0104002].
5. C. T. H. Davies *et al.*, Phys. Rev. Lett. **92**, 022001 (2004).
6. S. Durr, PoS **LAT2005**, 021 (2005) [arXiv:hep-lat/0509026].
7. M. F. L. Golterman and J. Smit, Nucl. Phys. B **255**, 328 (1985).
8. B. C. Tiburzi, Phys. Rev. D **72**, 094501 (2005).
9. J. A. Bailey and C. Bernard, PoS **LAT2005**, 047 (2005) [arXiv:hep-lat/0510006].
10. W. J. Marciano, Phys. Rev. Lett. **93**, 231803 (2004).
11. C. Aubin *et al.* [MILC Collaboration], Phys. Rev. D **70**, 114501 (2004).
12. D. Bećirević *et al.*, Nucl. Phys. B **705**, 339 (2005) [arXiv:hep-ph/0403217].
13. M. Okamoto [Fermilab Lattice Collaboration], arXiv:hep-lat/0412044.
14. C. Dawson *et al.*, PoS **LAT2005**, 337 (2005) [arXiv:hep-lat/0510018].
15. N. Tsutsui *et al.* PoS **LAT2005**, 357 (2005) [arXiv:hep-lat/0510068].
16. E. Blucher *et al.*, arXiv:hep-ph/0512039.
17. S. Eidelman *et al.*, [Particle Data Group], Phys. Lett. B **592**, 1 (2004).
18. I. Caprini, L. Lellouch and M. Neubert, Nucl. Phys. B **530**, 153 (1998).
19. S. Hashimoto *et al.*, Phys. Rev. D **61**, 014502 (2000).
20. M. Okamoto *et al.*, Nucl. Phys. Proc. Suppl. **140**, 461 (2005) [arXiv:hep-lat/0409116].
21. Heavy Flavor Averaging Group (HFAG), arXiv:hep-ex/0505100.
22. J. Laiho and R. S. Van de Water, arXiv:hep-lat/0512007.
23. J. M. Flynn *et al.* [UKQCD Collaboration], Nucl. Phys. B **461**, 327 (1996).
24. E. Gulez *et al.*, Phys. Rev. D **73**, 074502 (2006).
25. K. C. Bowler *et al.* [UKQCD Collaboration], Phys. Lett. B **486**, 111 (2000).
26. D. Bećirević and A. B. Kaidalov, Phys. Lett. B **478**, 417 (2000).
27. P. Ball and R. Zwicky, Phys. Rev. D **71**, 014015 (2005).
28. B. Aubert *et al.* [BABAR Collaboration], Phys. Rev. D **72**, 051102 (2005).
29. T. Hokuue [Belle Collaboration], arXiv:hep-ex/0604024.
30. For a review see H. D. Trottier, Nucl. Phys. Proc. Suppl. **129**, 142 (2004).
31. M. B. Oktay *et al.*, Nucl. Phys. Proc. Suppl. **129**, 349 (2004) [arXiv:hep-lat/0310016].
32. C. G. Boyd, B. Grinstein and R. F. Lebed, Phys. Rev. Lett. **74**, 4603 (1995).
33. L. Lellouch, Nucl. Phys. B **479**, 353 (1996).
34. P. B. Mackenzie, talk at FPCP 2006, <http://fpcp2006.triumf.ca/agenda.php>.
35. M. C. Arnesen *et al.*, Phys. Rev. Lett. **95**, 071802 (2005).
36. T. Becher and R. J. Hill, Phys. Lett. B **633**, 61 (2006).
37. For example, K. Abe *et al.* [BELLE Collaboration], arXiv:hep-ex/0408145.
38. C. Aubin *et al.*, Phys. Rev. Lett. **94**, 011601 (2005).

39. M. Wingate *et al.*, Phys. Rev. D **67**, 054505 (2003).
40. M. Ablikim *et al.* [BES Collaboration], Phys. Lett. B **597**, 39 (2004).
41. J. M. Link *et al.* [FOCUS Collaboration], Phys. Lett. B **607**, 233 (2005).
42. For recent quenched results see K. C. Bowler *et al.*, JHEP **0405**, 035 (2004).
43. S. B. Athar *et al.*, Phys. Rev. D **68**, 072003 (2003).
44. Discussion with C. Michael and J. Shigemitsu (2005).
45. C. Schwanda *et al.* [Belle Collaboration], Phys. Rev. Lett. **93**, 131803 (2004).
46. N. Isgur and H. B. Thacker, Phys. Rev. D **64**, 094507 (2001).
47. C. McNeile, C. Michael and K. J. Sharkey, Phys. Rev. D **65**, 014508 (2002).
48. C. Dawson, PoS **LAT2005**, 007 (2005).
49. R. Gupta, T. Bhattacharya and S. R. Sharpe, Phys. Rev. D **55**, 4036 (1997).
50. L. Lellouch and C.-J. D. Lin, Phys. Rev. D **64**, 094501 (2001).
51. C. Aubin and C. Bernard, Phys. Rev. D **73**, 014515 (2006).
52. A. Gray *et al.* Phys. Rev. Lett. **95**, 212001 (2005).
53. E. Gulez, J. Shigemitsu and M. Wingate, Phys. Rev. D **69**, 074501 (2004).
54. K. Ikado *et al.* [Belle Collaboration], arXiv:hep-ex/0604018.
55. C. Aubin *et al.*, Phys. Rev. Lett. **95**, 122002 (2005).
56. G. Bonvicini *et al.* [CLEO Collaboration], Phys. Rev. D **70**, 112004 (2004).
57. M. Artuso *et al.* [CLEO Collaboration], Phys. Rev. Lett. **95**, 251801 (2005).
58. A. Gray *et al.*, Nucl. Phys. Proc. Suppl. **140**, 446 (2005) [arXiv:hep-lat/0409040].
59. S. Aoki *et al.*, Phys. Rev. Lett. **91**, 212001 (2003).
60. M. Okamoto, PoS **LAT2005**, 013 (2005) [arXiv:hep-lat/0510113].
61. S. Hashimoto, Int. J. Mod. Phys. A **20**, 5133 (2005) [arXiv:hep-ph/0411126].
62. F. Gabbiani, E. Gabrielli, A. Masiero and L. Silvestrini, Nucl. Phys. B **477**, 321 (1996).
63. D. Bećirević *et al.*, JHEP **0204**, 025 (2002).
64. M. Guagnelli, F. Palombi, R. Petronzio and N. Tantalo, Phys. Lett. B **546**, 237 (2002).
65. J. Heitger and R. Sommer JHEP **0402**, 022 (2004).
66. H. W. Lin and N. H. Christ, PoS **LAT2005**, 225 (2005) [arXiv:hep-lat/0510111].
67. F. Palombi, M. Papinutto, C. Pena and H. Wittig, arXiv:hep-lat/0604014.
68. V. Abazov [D0 Collaboration], arXiv:hep-ex/0603029.
69. G. Gomez-Ceballos [CDF], at FPCP 2006, <http://fpcp2006.triumf.ca/agenda.php>.
70. M. Wingate *et al.*, Phys. Rev. Lett. **92**, 162001 (2004).
71. V. Gadiyak and O. Løktik, Phys. Rev. D **72**, 114504 (2005).
72. A. Lenz, arXiv:hep-ph/0412007.
73. N. Yamada *et al.*, Nucl. Phys. Proc. Suppl. **106**, 397 (2002) [arXiv:hep-lat/0110087].
74. K. Abe *et al.*, arXiv:hep-ex/0506079.
75. For recent efforts, see D. Bećirević, arXiv:hep-ph/0211340.
76. S. Hashimoto and H. Matsufuru, Phys. Rev. D **54**, 4578 (1996).
77. J. H. Sloan, Nucl. Phys. Proc. Suppl. **63**, 365 (1998) [arXiv:hep-lat/9710061].
78. K. M. Foley and G. P. Lepage, Nucl. Phys. Proc. Suppl. **119**, 635 (2003).
79. K. M. Foley *et al.*, Nucl. Phys. Proc. Suppl. **140**, 470 (2005).
80. A. Dougall, K.M. Foley, C.T.H. Davies and G.P. Lepage, PoS **LAT2005**, 219 (2005).
81. B. Aubert *et al.* [BABAR Collaboration], Phys. Rev. Lett. **91**, 221802 (2003).
82. A. Ishikawa *et al.* [Belle Collaboration], Phys. Rev. Lett. **91**, 261601 (2003).
83. B. Aubert [BABAR Collaboration], arXiv:hep-ex/0604007.
84. E.g. A. Ali, P. Ball, L. T. Handoko and G. Hiller, Phys. Rev. D **61**, 074024 (2000).
85. M. Neubert and C. T. Sachrajda, Nucl. Phys. B **483**, 339 (1997).
86. D. Bećirević, arXiv:hep-ph/0110124.
87. M. B. Voloshin, Phys. Lett. B **515**, 74 (2001).
88. I. F. Allison, *et al.*, Phys. Rev. Lett. **94**, 172001 (2005).

16 *Matthew Wingate*

89. D. Acosta *et al.* [CDF Collaboration], arXiv:hep-ex/0505076.